



Exploring the Metal Sensing Capability of Tetrazole Hydrazide Schiff base

**B. ANUPAMA^{1*}, AMEENA HUSAIN², SUNITHA MUNAGALA³, ZAAKIYA MARYAM OSMANI⁴,
GOLI BHARGAVI⁵ and P.S.S INDIRA PRIYA DARSHINI⁶**

^{1*}Department of Chemistry, RBVRR Women's College, Narayanaguda, Hyderabad, Telangana, India.

^{2,4,5,6}Department of Chemistry, VCIWU, Koti, Hyderabad, Telangana, India.

³Government Polytechnic, Nalgonda Hyderabad, Telangana, India.

*Corresponding author E-mail: anupamagudi62@gmail.com

<http://dx.doi.org/10.13005/ojc/420114>

(Received: July 07, 2025; Accepted: September 13, 2025)

ABSTRACT

Tetrazole ring based salicylaldehyde Schiff base, 2-Hydroxy Phenyl Methylidene-2-1H-Tetrazol-5-yl-Aceto-hydrazide was prepared by Microwave assisted synthesis and characterized by Mass, UV-Vis, Infrared, ¹H-NMR and TG-DTA techniques. Thermogravimetric analysis suggested its explosive property. Its metal sensing capability was investigated against 14 different metal ions (Ba²⁺, Cd²⁺, Co²⁺, Fe²⁺, K⁺, Mn²⁺, Ni²⁺, Pb²⁺, Zn²⁺, Na⁺, Mg²⁺, Al³⁺, Cu²⁺ and Hg²⁺). The results were analyzed by Visual, UV-Vis and Fluorescence spectral techniques. Visual analysis showed pale yellow colored TSB+Fe solution in contrast to all other colorless TSB+metal solutions. Considerable hyperchromic shift occurred for Pb and Fe in UV-Vis spectra. Bathochromic shift and Quenching were seen for these two cations in addition to Na & Mg in Fluorescence spectrum. Therefore, TSB has the propensity to function as an efficient metal sensor for Pb, Fe, Na and Mg.

Keywords: Bathochromic shift, Explosive, Fe²⁺, 2-Hydroxy phenyl methylidene-2-1H-Tetrazol-5-yl-Aceto-hydrazide, Pb²⁺, Hyperchromic shift, Quenching.

INTRODUCTION

The tetrazole ring was first prepared by a Swedish scientist named Bladin, in 1885. This nitrogen rich heterocycle behaves as a polydentate ligand¹ having an N-acyl hydrazone scaffold. Such scaffolds are useful to medicinal chemists during drug discovery and development processes². This scaffold is also bioisosteric with amide bond³. This ring has found versatile applications as competent ligands and energetic materials⁴. Its resistance to metabolic degradation makes it a promising contender for many studies including biological

activity studies⁵. This heterocyclic ring is highly preferred for preparing efficient luminescent substances, due to intra ligand n→π* and π→π* transitions. The photochemistry of tetrazole ring is influenced by the extended groups attached to it⁶.

Azomethines are well recognized scaffolds for their multifunctional applications. TSB contains multiple donor sites for coordinating with metal ions (Fig. 1). These include Phenolic (-OH), azomethine (-C=NH), carbonyl group (C=O) and Pyrrole type -NH of tetrazole ring. This ring -NH is allosteric with -COOH^{3,7,8,9}. The role of Schiff bases as metal sensors



has gained popularity in recent past due to their color properties, multifunctionality, stability, solubility and coordination ability^{10,11,12}. Musa Kamaci¹³ has reported in detail, the role of poly azomethine urethanes as efficient fluorescent Cr³⁺ chemo sensor.

Numerous analytical practices have been established and reported for metal ion detection, like Voltammetry, Gravimetry, Chromatography, Colorimetry, ICP-MS, Flame photometry etc.¹⁴⁻²¹. Some of these techniques are facile, with easy-to-handle instruments, whereas others may require exhausting multistep procedures. In current investigation we have used UV-Vis and Fluorescence techniques for exploring the metal sensing propensity of TSB.

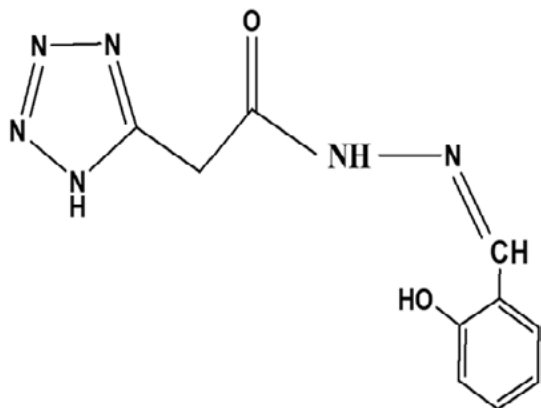
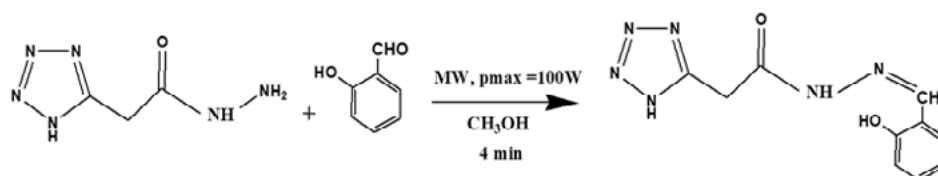


Fig. 1. Structure of 2-Hydroxy phenyl methylidene -2-1H-tetrazole-5-yl-Acetohydrazide



Scheme 1. MW assisted synthesis of TSB

Preparation of the Stock Solutions

A 0.1mM solution of TSB was prepared in DMF. The aqueous solutions of metal cations (0.1mM) such as Ba²⁺, Cd²⁺, Co²⁺, Fe²⁺, K⁺, Mn²⁺, Ni²⁺, Pb²⁺, Zn²⁺, Na⁺, Mg²⁺, Al³⁺, Cu²⁺ and Hg²⁺ were prepared in deionized water by using their chloride, nitrate or sulphate salts.

Metal Sensor Studies

A 0.1mM solution of TSB in DMF was mixed with metal cation (0.1mM) solutions (Ba²⁺, Cd²⁺, Co²⁺, Fe²⁺, K⁺, Mn²⁺, Ni²⁺, Pb²⁺, Zn²⁺, Na⁺, Mg²⁺, Al³⁺, Cu²⁺ and Hg²⁺) in deionized water in 1:1 M ratio. The results were analyzed visually and spectrophotometrically. The pH

EXPERIMENTAL

MATERIALS AND METHODS

All the chemicals were procured from Merck. The solvents used were distilled and then used for the experimental purpose. IR spectrum was recorded on Bruker FT-IR spectrometer (4000-400 cm⁻¹ range). Proton NMR spectra of ligands were recorded on Bruker 400MHz Ultrashield Spectrometer by using solvent DMSO-d₆. LCMS Spectra were recorded on 2010A SHIMADZU instrument. Metal sensor experiments were done on Shimadzu UV-Vis spectrometer (model1800) and Shimadzu Spectrofluorimeter (RF 5301 PC).

Microwave assisted synthesis of TSB

2-(1H-Tetrazol-5-yl) acetohydrazide (1 eq) and salicylaldehyde (4 eq) were suspended in 6 mL methanol. The reaction mixture was heated by microwave irradiation (p_{max} = 100 W, ramp time = 1 min, hold time = 2 minutes). This product was cooled to room temperature then stirred in ice-salt bath for 30 minutes. The resultant bright yellow TSB ligand was separated and purified with water and alcohol, and then dried in oven. Product yield is 85%. Melting Point: 248-250°C (reported 250^o-251^o C) (Scheme 1)²².

was maintained between 6-11 as this was found to be most effective pH range for detection of metal ions.

RESULTS AND DISCUSSION

Physical properties of TSB

The ligand TSB exists as stable yellow solid at room temperature. It was soluble in methanol, DMSO and DMF.

Characterization of TSB

It was characterized by Mass spectrometry, Electronic, Infrared and H¹-NMR spectral techniques and TG-DTA.

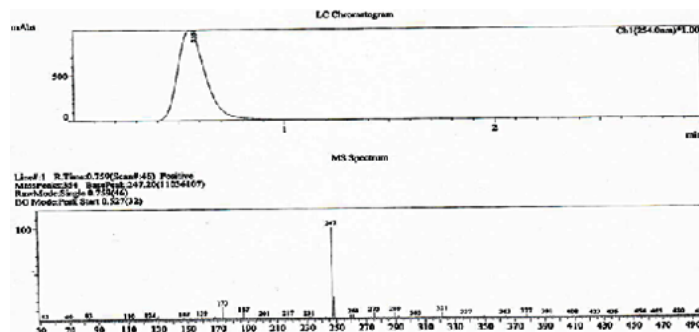


Fig. 2. LCMS of TSB

Mass Spectral Data of TSB

The LCMS of the TSB showed signal at 247 [M+2] m/z consistent with its calculated weight i.e. 245 (Figure 2).

IR Spectral Studies

In IR spectrum of TSB, weak-O-Hstr band appearing in the range 3000-2500 cm^{-1} is attributable to intramolecular H-bonded phenolic -OH. The -CH₂- group vibrations observed as weak bands at 2848 cm^{-1} and 2947 cm^{-1} are due to asymmetric and symmetric stretching respectively. Bands at 1392 & 1322 cm^{-1} (range 1390-1330 cm^{-1}), 1262 and 1204 cm^{-1} (range 1260-1180 cm^{-1}) are probably due to coupling of O-H bending and C-O stretching modes of vibrations of phenolic moiety. In the spectrum $\nu_{\text{C=O}}$ appeared as intense band at 1676 cm^{-1} (literature 1674 cm^{-1}) and the $\nu_{\text{C=N}}$ appeared at 1610 cm^{-1} (literature 1604 cm^{-1})²². The appearance of strong C-H_{oop} bending vibration between 770-730 cm^{-1} confirms presence of ortho substituted benzene in TSB. (Figure 3, Table 1).

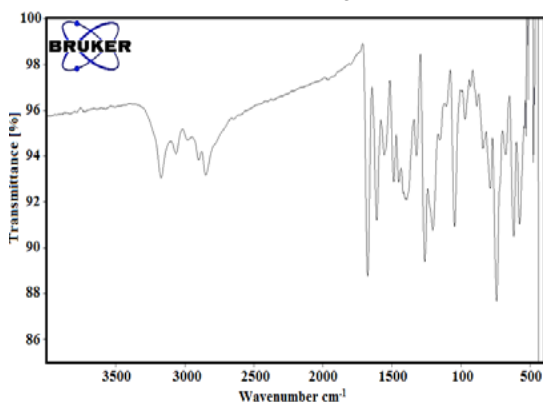


Fig. 3. IR Spectrum of TSB

Table 1: IR spectral data of TSB

Ligand	N-H _{str}	O-H _{str}	C-H _{str} -CH ₂ -	C=O _{str}	C=N Azomethine	C-O _{str}	C-H _{oop}
TSB	3200	3173	2848	1676	1610	1262	742

UV-Visible Spectral Studies of TSB

TSB displays three signals between 290–360nm. High intensity band at 293nm arises due to allowed $\pi \rightarrow \pi^*$ transitions, low absorbance band at 340nm appears owing to forbidden $n \rightarrow \pi^*$ transitions and band at 356nm arises from intramolecular charge transfer transitions (Figure 4, Table 2)

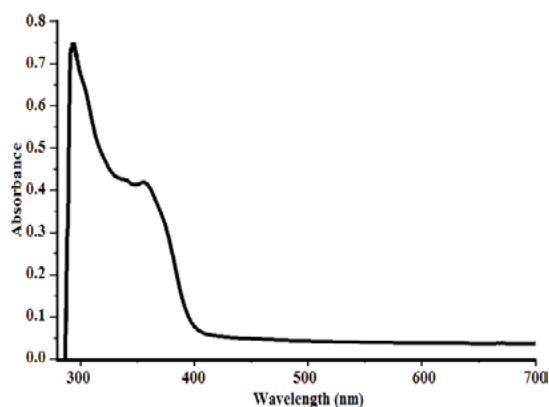


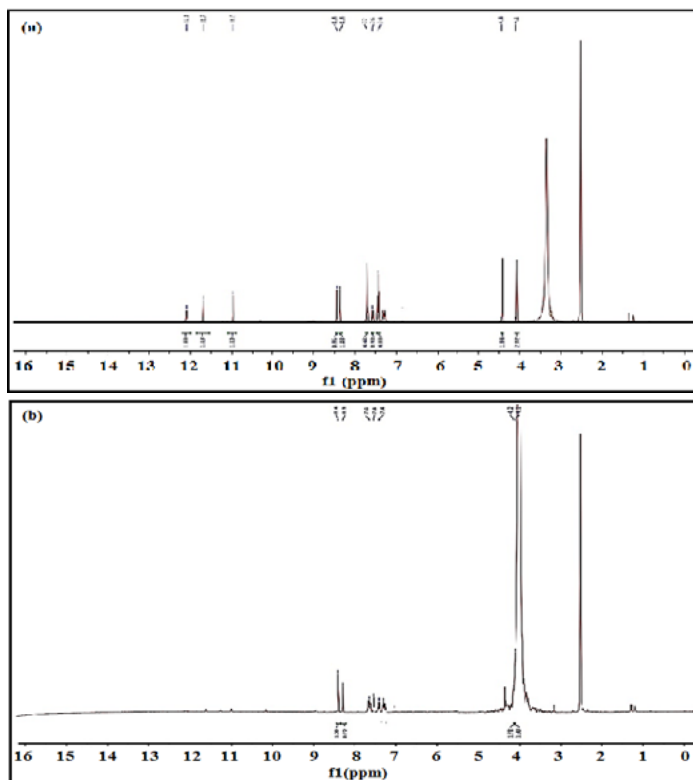
Fig. 4. UV-Vis Spectrum of TSB

Table 2: UV-Vis spectral data of TSB

Ligand	Solvent	Absorption region(nm)	Band assignment
TSB	DMF	293	$\pi \rightarrow \pi^*$
		341	$n \rightarrow \pi^*$
		356	CT

¹H-NMR Analysis of TSB

¹H-NMR of TSB was recorded DMSO-d₆, duplication of peaks was observed for NH, N=CH, CH₂ and aryl protons (Fig. 5(a)). The CH₂ group gave two, equal intensity, singlets at δ 4.1 & δ 4.5. The -NH also gave two singlets of unequal intensities at δ 11.7 & δ 12.1²³. The signals from -OH & -NH disappeared upon D₂O exchange (Fig. 5(b)). The aryl protons appeared in the region δ 7.4-7.6. The azomethine protons appeared at δ 8.4 & δ 8.43. The data is recorded in Table 3.

Fig. 5. NMR spectra of TSB in solvent DMSO-d₆ (a) ¹H-NMR (b) D₂OTable 3: ¹H-NMR data (δ) of TSB in solvents DMSO-d₆

Solvent	-CH ₂ -	N=CH	CONH(D ₂ O)	Aromatic protons	-OH(D ₂ O)
DMSO	4.4, 4.1	8.4, 8.43	11.7, 12.1	7.4-7.6	11.0

TGA-DTA analysis of TSB

TGA-DTA analysis was executed for nitrogen rich tetrazole ring-based TSB to determine the existence of explosive property, if present. These results are tabulated in Table 4.

TGA-DTA thermogram of TSB showed five events of weight loss (Fig. 6). Initial endothermic weight loss at 221.8°C may be attributed to its melting, followed by another endothermic loss at 265.8°C. Subsequent exothermic weight losses were observed at 285.2°C and a major loss at 578.8°C. Lastly one minor endothermic loss occurred at

727.0°C. The T_{endo→exo} at 265.8°C indicates explosive decomposition of TSB¹. This explosive behavior may be attributed to presence of electron withdrawing azomethine, carbonyl groups and electron donating ring & hydrazide nitrogen within the same molecule.

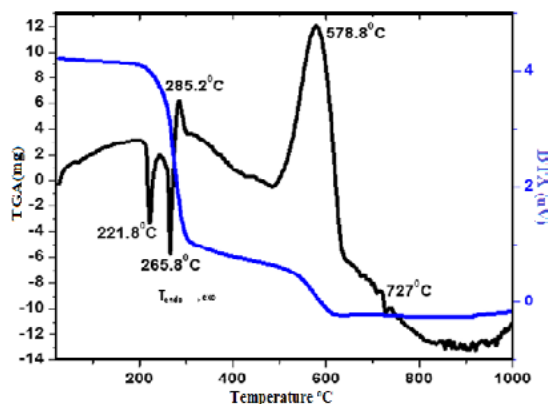


Fig. 6. TGA and DTA curves of TSB

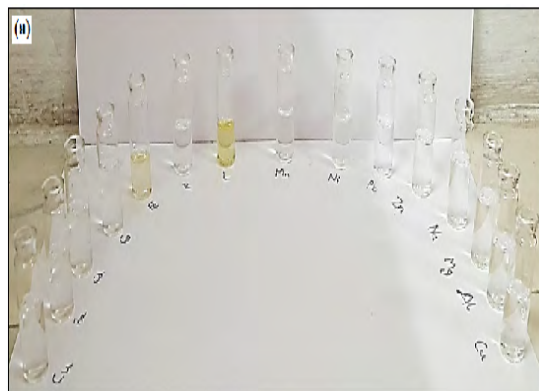
Table 4: TGA-DTA data of TSB

Ligand	Temperature (°C)	Loss in weight Found (cal)%	Probable composition of expelled groups
TSB C ₁₀ H ₁₀ N ₆ O ₂	221.8	7.7 (7.8)	OH, H ₂ C ₅ H ₂ N ₃ O C ₄ N 4N
	265.8	39 (38.9)	
	285.2	25.2 (24.8)	
	578.8	Weight loss is negative due to explosive decomposition	

Metal Sensing Studies

Visual Method

Upon mixing yellow colored 0.1 mM TSB with colorless 0.1 mM cation solutions of 14 different



metals, all the solutions turned colorless except TSB+Fe²⁺, which appeared pale yellow (Fig. 7). Therefore, TSB is found to be an efficient visual sensor for Fe²⁺.

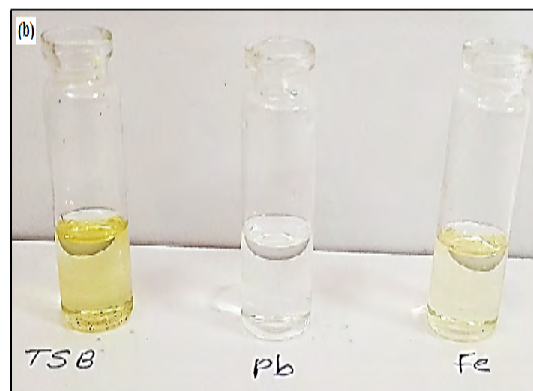


Fig. 7. Visual analysis of TSB+Metal ions (a) & (b)

UV-Vis Sensor Studies

The metal sensing ability of TSB was investigated by recording the absorbance of TSB+14 different metal solutions mixed in 1:1 ratio. The nascent TSB excitations were observed at λ_{\max} 300 & 353nm having ϵ_{\max} of 0.244 and 0.129 respectively. These may be ascribed to $\pi \rightarrow \pi^*$ and

$n \rightarrow \pi^*$ transitions respectively. After mixing TSB with metal solutions, no significant variations were detected for most metal solutions, except Pb²⁺ and Fe²⁺ (Fig. 8). Addition of these two metals led to distinct hyperchromic shift with isosbestic points. Thus, TSB functions as an effective UV-Vis sensor for Fe and Pb detection.

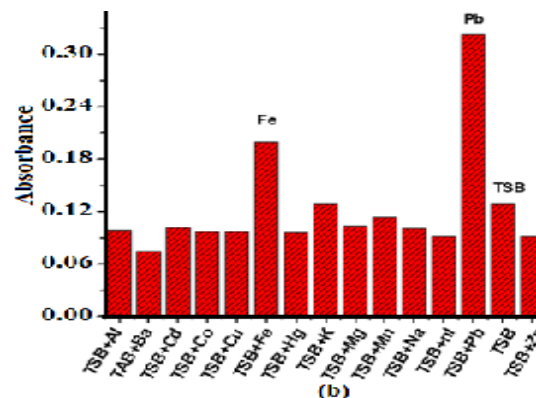
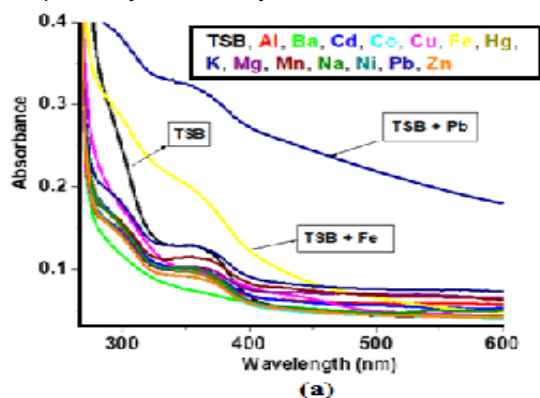


Fig. 8. Graphs showing metal sensing ability of TSB (a) UV-Vis spectrum (b) Bar Graph

Fluorescence Sensor Studies

The fluorescence studies of TSB showed two strong emissions at 419nm and 438nm when excited at 350nm. The intensities were 62.3 and 85.6 respectively. Addition of metal ions resulted in bathochromic shift of approximately 5-7nm with quenching. These may be due to coordination of the azomethine group, phenolic -OH, ring -NH and C=O groups with the metal ions. Quenching was maximum for Fe+TSB (Intensity 18.4) solution. Though most of the emissions overlapped, clear bands were visible for Na, Mg, Pb & Fe (Figure 9).

Practical utility

Lead is a well-known toxicant. Sources of lead pollution include urban soil waste, poor quality paints and dyes, factory chimneys, melting and casting of ores, wastes from storage battery industries, metal plating and related industries, fertilizers, pesticides and gasoline additives etc. Exposure to unhealthy levels of lead has been interrelated to anemia, kidney ailments, reproductive problems in adults, learning difficulties in children including speech and behavioral issues.

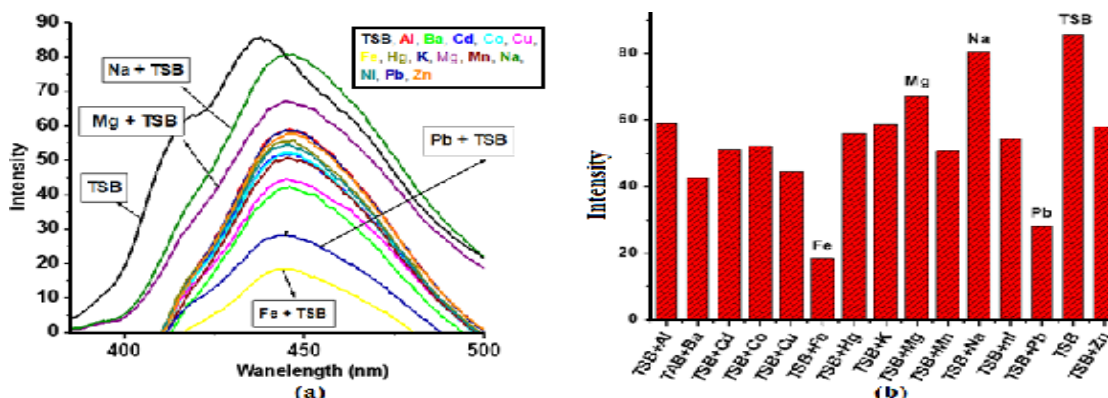


Fig. 9. Graphs showing metal sensing ability of TSB (a) Fluorescence spectrum (b) Bar Graph

Iron is most widely used metal and has found many applications in motor industry, steel industry, machines, pipelines, military equipment, appliances etc. But years of iron ore mining has led to pollution of air, surface and ground water, flora and fauna¹⁴. Iron based nanoparticles released in water bodies are toxic to bacteria, algae, fish and plants²⁴. Salt has been used as an effective deicer, as it causes freezing point depression. But years of use of millions of tons of salt has endangered the flora and fauna of fresh water bodies and contaminated drinking water wells. Harsha et al have incorporated a polymer-imidazole based sensor on a glass slide and used it as a simple yet cost effective Cu^{2+} detector¹¹.

The 11th and 12th Principle of green chemistry, as quoted by Prof Paul Anastas, states "Monitor chemical reactions in real-time as they occur to prevent the formation and release of any potentially hazardous and polluting substances" and "Choose and develop chemical procedures that are safer and inherently minimize the risk of accidents. Know the possible risks and assess them beforehand", respectively.

The above-mentioned concerns (and many not mentioned here) signify the need for cheap, facile and yet sensitive metal sensors and also serious conscious efforts by individuals and organizations to protect earth from indiscriminate pollution.

CONCLUSION

2-Hydroxy Phenyl Methylidene-2-1H-tetrazole-5-yl-Aceto-hydrazone was prepared by Microwave method and characterized by Mass Spectrometry, UV-Vis, Infrared and $^1\text{H-NMR}$ spectral

techniques. TG-DTA analysis was performed to discover the explosive nature of this nitrogen rich heterocycle. Metal sensing ability of TSB against 14 different cations (Ba^{2+} , Cd^{2+} , Co^{2+} , Fe^{2+} , K^+ , Mn^{2+} , Ni^{2+} , Pb^{2+} , Zn^{2+} , Na^+ , Mg^{2+} , Al^{3+} , Cu^{2+} and Hg^{2+}) was analyzed by visualization with naked eye, absorption changes and emission changes. All TSB+M solutions appeared colorless except TSB+Fe, which appeared pale yellow. Considerably distinct absorption bands appeared for TSB+Fe and TSB+Pb in UV-Vis spectrum. Noticeable decrease in fluorescence intensity was observed for Na, Mg, Pb and Fe when mixed with TSB. Hence it can be summarized that the presence of donor sites like, ring N-H, C=O, CH=N and phenolic OH groups make TSB an efficient ligand for coordinating with metals. It can detect Fe ions upon visual mixing, detect Fe and Pb using UV Visible spectrophotometer and Na, Mg, Pb and Fe using spectrofluorimeter.

ACKNOWLEDGEMENT

Authors would like express gratitude to Management of RBVRR Women's College, Hyderabad, for providing Seed Money for Minor Research Project to carry out this work and also acknowledge the management for establishing Central Research Instrumentation Laboratory in the College with CPE Funds, Shimadzu Spectrofluorometer (RF 5301 PC) and UV-Vis spectrophotometer (Schimadzu model 1800). Authors are also grateful to CFRD, Osmania University, Hyderabad (NMR). Research Lab-1, VCIWU, Hyderabad, for the facilities provided.

Declaration

The authors declare that there is no conflict of interests regarding the publication of this article.

REFERENCES

1. Wurzenberger, M.H.H.; Gruhne, M. S.; Lommel, M. and Stierstorfer., *J. Propellants, Explosives, Pyrotechnics.*, **2022**, *46*, 207–213. <https://doi.org/10.1002/prep.202000179>
2. Yamazaki, D.A.; Rozada, A. M.; Barea, P.; Reis, E. C.; Basso, E. A.; Sarragiotto, M. H.; Seixas, F. A. and Gauze, G.F., *Bioorganic & Medicinal Chemistry.*, **2021**, *32*, 115991. <https://doi.org/10.1016/j.bmc.2020.115991>
3. Pedreira, J. G.; Nahidino, P.; Kudolo, M.; Pantsar, T.; Berger, B.T.; Forster, M.; Knapp, S.; Laufer S. and Barreiro, E. J., *J. of Medicinal Chemistry.*, **2020**, *63*, 7347-7354. <https://doi.org/10.1021/acs.jmedchem.0c00508>
4. Kofen, M.; Lommel, M.; Wurzenberger, M. H. H.; Klapötke T. M. and Stierstorfer, J., **2022**, *28*, e202200492. <https://onlinelibrary.wiley.com/doi/pdf/10.1002/chem.202200492>
5. Narang, R.; Narasimhan, B. and Sharma, S., *Current Medicinal Chemistry.*, **2012**, *19*, 569-612. <http://dx.doi.org/10.2174/092986712798918789>
6. Pagacz-Kostrzewa, M.; Krupa, J. and Wierzejewska, M., *Journal of Physical Chemistry A.*, **2014**, *118*, 2072–2082. <https://doi.org/10.1021/jp5001804>
7. Rìger, N.; Roatsch, M.; Emmrich, T.; Franz, H.; Schile, R.; Jung, M. and Link, A. *ChemMedChem.*, **2015**, *10*, 1875–1883. <https://doi.org/10.1002/cmcd.201500335>
8. Ornstein, P. L.; Schoepp, D. D.; Arnold, M. B.; Jones, N. D.; Deeter, J. B.; Lodge, D. and Leander, J. D., *Journal of Medicinal Chemistry.*, **1992**, *35*, 3111-3115. <https://pubs.acs.org/doi/10.1021/jm00095a004>
9. Lunn, W.H.W.; Schoepp, D. D.; Calligaro, D. O.; Vasileff, R. T.; Heinz, L. J.; Salhoff, C. R. and O'Malley, P. J., *Journal of Medicinal Chemistry.*, **1992**, *35*, 4608-4612. <https://doi.org/10.1021/jm00102a015>
10. Anupama B., *J. of Indian Chemical Society.*, **2020**, *97*, 721-724. <https://indianchemicalsociety.com/portal/uploads/journal/May-2.pdf>
11. Harsha, K.G.; Appalanaidu, E.; Rao, B. A.; Baggi, T. R. and Rao, V. J., *Russian J. of Organic Chem.*, **2020**, *56*, 158–168. <https://link.springer.com/article/10.1134/S1070428020010248>
12. Tomer, N.; Goel, A.; Ghule V. D. and Malhotra, R., *Journal of Molecular Structure.*, **2021**, *1227*, 129549. <https://doi.org/10.1016/j.molstruc.2020.129549>
13. Musa, K., *J. of Fluorescence.*, **2023**, *33*, 53-59. <https://doi.org/10.1007/s10895-022-03037-7>
14. Gleekia, A.M.G.D.; Pradhan, D. S. and Sahu, H. B. Conference: Geomintech Symposium: New Equipment New Technology- Management and Safety in Mines and Mineral Based Industries, Bhubaneswar, India., **2016**, *IV(2)/Q2*. https://www.researchgate.net/publication/304580575_IMPACTS_OF_IRON_ORE_MINING_ON_WATER_QUALITY_AND_THE_ENVIRONMENT_IN_LIBERIA
15. Fu, J.; Li, B.; Mei, H. Chang, Y. and Xu, K., *Spectrochemical Acta Part A: Mol. Biomol. Spectrosc.*, **2020**, *227*, 117678. <https://doi.org/10.1016/j.saa.2019.117678>
16. Liu, L.W.; Zheng, H. L.; Xu, B. C.; Xiao, L.; Chigan, Y. and Zhangluo, Y.L., *Talanta.*, **2018**, *179*, 86–91. <https://dx.doi.org/10.1016/j.talanta.2017.10.003>
17. Eang, P.; Fu, J. X.; Yao, K.; Chang, Y. X.; Xu, K. X. and Xu, Y. Q., *Actuators B Chem.*, **2018**, *273*, 1070–1076. <https://doi.org/10.1016/j.snb.2018.07.028>
18. Li, Q.; Zhang, Z. and Wang, Z., *Anal. Chim. Acta.*, **2014**, *845*, 7–14. <https://doi.org/10.1016/j.snb.2017.01.149>
19. Li, S.Y.; Zhang, D.B.; Wang, J.Y.; Lu, R. M.; Zheng, C. H. and Pu, S. Z. *Sen. Actuators. B.*, **2017**, *245*, 263–272. <https://doi.org/10.1016/j.jallcom.2020.154357>
20. Dong, Y.; Zhou, M. and Zhang, L., *J. Alloys Compd.*, **2020**, *827*, 154357. <https://doi.org/10.1016/j.jallcom.2020.154357>
21. Yamini Y.; Alizadeh, N. and Shamsipur, M., *Anal. Chim. Acta.*, **1997**, *355*, 69–74. [https://doi.org/10.1016/S0003-2670\(97\)81613-3](https://doi.org/10.1016/S0003-2670(97)81613-3)
22. Riger, N.; Fassauer, G. M.; Bock, C.; Emmrich, T.; Bodtke, A. and Link, A., *Mol Divers.*, **2017**, *9*, 9-27. PMID: 28028725. <https://doi.org/10.1007/s11030-016-9711-x>
23. Munir, R.; Javid, N.; Zia-ur-Rehman, M.; Zaheer, M.; Huma, R.; Roohi, A. and Athar, M. M., *Molecules.*, **2021**, *26*, 4908. <https://www.mdpi.com/1420-3049/26/16/4908#>
24. Lei, C.; Sun, Y.; Tsang, D. C. W. and Lin, D., *Environmental Pollution.*, **2017**, *232*, 10-30. <https://doi.org/10.1016/j.envpol.2017.09.052>